

**Monitoring and Modulating the Catalytic Hybridization Circuit for
Self-Adaptive Bioorthogonal DNA Assembly**

Xue Gong ‡, Shizhen He‡, Ruomeng Li‡, Yingying Chen, Kaiyue Tan, Yeqing Wan,

*Xiaoqing Liu, Fuan Wang**

College of Chemistry and Molecular Sciences, Wuhan University, Wuhan, P. R.

China

*To whom correspondence should be addressed. E-mail: fuanwang@whu.edu.cn.

‡These authors contributed equally to this work

Table of Contents

Experimental section	S2
Table S1. The DNA sequences used to construct LCC system	S10
Figure S1. Schematic illustration the miR-21-responsive LCC system.....	S11
Figure S2. The feasibility of the miR-21 sensing platform.....	S12
Figure S3. Comparison of the assembly efficiency	S13
Figure S4. Diffusion coefficient assay at different conditions.....	S14
Figure S5. AFM characterization	S15
Figure S6. Stability of the DNA hydrogel.....	S16
Figure S7. Schematic illustration the synthesized PLGA-PEG-FA.....	S17
Figure S8. ¹ H NMR spectra	S18
Figure S9. Stability evaluation of the FA-nanovesicle	S19
Figure S10. The biocompatibility evaluation of the FA-nanovesicle	S20
Figure S11. Inhibition analysis in FR-positive MCF-7 cells	S21
Figure S12. Inhibition analysis in FR-negative MCF-10A cells.....	S22
Figure S13. Inhibition analysis in FR-positive HeLa cells	S23
Figure S14. Cellular uptake mechanism of the FA-nanovesicles	S24
Figure S15. Optimization of incubation time.....	S25
Figure S16. Flow cytometric analysis of miR-21 in living MCF-7 cells	S26
Figure S17. Diffusion coefficient assay in MCF-7 cells.....	S27
Figure S18. Signal intensities of major tissues and tumours	S28
Figure S19. H&E staining of major organs.....	S29
Figure S20. Biosafety evaluation of the FA-decorated nanovesicles in vivo	S30
References	S31

Experimental section

Materials and Reagents.

All oligonucleotides were synthesized and HPLC-purified by Sangon Biotechnology Co., Ltd. (Shanghai, China), and the sequences are listed in **Table S1**. Poly (lactic-co-glycolic acid) (Resomer® RG502H monomer ratio 50:50, MW 7-17 kDa), Polyvinyl alcohol (PVA, 80% hydrolyzed, MW 9-10 kDa), poly-L-lysine hydrobromide (PLL, MW 30,000-70,000) were purchased from Sigma-Aldrich. NH₂-PEG-NH₂ (MW:2000) was obtained from Xi'an ruixi Biological Technology Co., Ltd (China). Dulbecco's modified Eagle's medium (DMEM), fetal bovine serum (FBS), trypsin, penicillinstreptomycin, Dulbecco's phosphate buffered saline (PBS), and Hoechst 33342 were all obtained from Thermo Fisher. Anti-PDCD4 and anti-PTEN were both acquired from Abcam Biosciences (USA), while anti-GAPDH was purchased from Cell Signaling Technology (USA). Atomic force microscope (AFM) cantilever (SCANASYST-AIR) was purchased from Bruker (Camarilla, CA). Other reagents were of analytical grade and were used without further purification. All solutions were prepared using ultrapure water, which was obtained through a Millipore Milli-Q water purification system with an electric resistance >18.2 MΩ·cm.

Construction of the LCC system for signal amplification.

Each DNA hairpin was diluted in HEPES buffer (10 mM HEPES, 1 M NaCl, 50 mM MgCl₂, pH 7.2) at 4 μM final concentrations and annealed at 95 °C for 5 min, then quickly cooling down to 4 °C in 30s. For amplified detection of analyte by using the LCC amplifier, miRNA was introduced into the **H₁+H₂+H₃** mixtures (200 nM each) to initiated the localized hybridization at 25 °C. Subsequently, time-dependent fluorescence measurements were performed and monitored on a Cary Eclipse fluorescence spectrophotometer (Varian Inc). The emission spectra were acquired by exciting the samples at 490 nm, and fluorescence spectra were collected from 505 to 650 nm.

FCS Measurements.

FCS measurements were performed on a Leica TCS SP8 confocal laser scanning microscope with a 63×1.2 NA water immersion objective. DNA hydrogels labeled with Alexa Fluor 488 in solutions or cells were excited by selecting the 488 nm laser line with a pulse frequency of 40 MHz, and fluorescence spectra were collected from 495 to 525 nm. FCS data was analyzed by Symphotime 64 software, using a three-dimensional (3D) diffusion model. In FCS, the intensity fluctuations can be correlated with an autocorrelation function as follows:

$$G(\tau) = \frac{\langle \delta F(t) \times \delta F(t + \tau) \rangle}{\langle F(t) \rangle^2}$$

where $G(\tau)$ is the normalized fluorescence fluctuation autocorrelation function, $\langle F \rangle$ is the average intensity and $\delta F(\tau)$ is the fluctuation in intensity at a delay τ around the mean value.

By using a three-dimensional (3D) diffusion model, the autocorrelation function can be fitted to a single-component model equation:

$$G(\tau) = 1 + N_{eff}^{-1} \times \left(1 + \frac{\tau}{\tau_D}\right)^{-1} \times \left(1 + S^2 \cdot \frac{\tau}{\tau_D}\right)^{-1/2}$$

where N_{eff} is the average number of particles in the effective measurement volume element V_{eff} , τ_D is the characteristic diffusion time and S is the structural parameter [$S = \text{waist } (w_0)/\text{axial radius } (z)$].

If the diffusion coefficient (D) and the concentration are known, the diffusion constant (D) can be calculated from the following equation:

$$\tau_D = \frac{w_0^2}{4D}$$

Electrophoresis.

For DNA samples used for gel electrophoresis assay, 100 nM of initiators were incubated with 400 nM hairpin mixtures ($H_1+H_2+H_3$) in reaction buffer (10 mM HEPES, 1 M NaCl, 50 mM MgCl₂, pH 7.2) for 4 h at 25 °C. Then, the prepared different samples were loaded into freshly prepared 8% native polyacrylamide gel and run at a

constant voltage of 150 V for 3 h in 1×TBE buffer (89 mM Tris, 89 mM Boric Acid, 2.0 mM EDTA, pH 8.3). The gel was then stained with GelRed and imaged by FluorChem FC3 (ProteinSimple, USA) under 365 nm UV irradiation.

Atomic force microscopy (AFM) characterization.

To distinguish the morphology of the assembled products, the DNA sample was prepared in reaction buffer (10 mM HEPES, 1 M NaCl, 50 mM MgCl₂, pH 7.2) that contained **H₁+H₂+H₃** (20 nM each) and miRNA (2 nM). The DNA sample was diluted and deposited on the modified mica for 15 min to allow its adsorption on the mica surface, followed by its rinsing with ultrapure water and drying under a stream of nitrogen. Then, the prepared sample was scanned in tapping mode by Multimode 8 Atomic Force Microscope with a NanoScope V controller (Bruker Inc.).

Rheological Measurement.

For mechanical characterizations, DNA hydrogel sample with a volume of 100 μL was loaded onto DHR-2 rheometer (TA Instruments). Oscillatory strain (0.01-1000%) and frequency sweep (0.01-100 Hz) tests were performed with a 20 mm parallel-plate geometry (with a gap size of 0.2 mm).

Synthesis of the amine-terminated diblock copolymer (PLGA-PEG-NH₂).

Amine-terminated diblock copolymer (PLGA-PEG-NH₂) was prepared according to literature report.^{1,2} In brief, PLGA-COOH (700 mg, 41.2 nmol) and a 4 molar excess of NHS (18.952 mg, 0.1648 mmol) and DCC (33.95 mg, 0.1648 mmol) were dissolved in anhydrous methylene chloride. The reaction mixture was stirred under nitrogen atmosphere for 24 h at room temperature for activation of carboxylic group of PLGA-COOH. The activated PLGA dissolved in anhydrous dichloromethane was added dropwise to five-times molar excess of PEG-bis amine dissolved in anhydrous DCM. A catalytic amount (100 μL) of anhydrous triethylamine was added to the mixture with gentle stirring. The reaction mixture was stirred under stirred under N₂ atmosphere for

24 h at room temperature. The reaction was quenched by adding ice-cold diethyl ether to the reaction mixture. The resultant precipitated product, PLGA-PEG-NH₂ was repeatedly washed with methanol to remove unreacted PEG-bis-amine and finally dried under vacuum.

Synthesis of the FA-coupled deblock copolymer (PLGA-PEG-FA).

The FA-conjugated deblock copolymer (PLGA-PEG-FA) was synthesized by coupling activated FA with the previously synthesized PLGA-PEG-NH₂ diblock copolymer. Briefly, 500 mg PLGA-PEG-NH₂ dissolved in 5 ml anhydrous dimethyl sulfoxide (DMSO) was mixed with FA (13 mg, 0.029 mmol), N, N'-dicyclohexylcarbodiimide, (8.96 mg, 0.0435 mmol) and 100 μ L anhydrous triethylamine. The reaction was stirred under N₂ atmosphere for 24 h at room temperature. Then, the reaction mixture was filtered and the filtrate was added dropwise into ice cold diethyl ether to obtain a precipitate of PLGA-PEG-FA, the precipitate was separated by filtration, repeatedly washed with methanol to remove DMSO and finally dried under vacuum. Noteworthy, the unconjugated FA was removed by dissolving conjugated diblock copolymer in DCM; FA being insoluble in DCM was removed by filtration.

The preparation of FA-nanovesicle.

FA-decorated nanovesicle was synthesized by the conventional double emulsion solvent evaporation method.³ Briefly, an excess of PLL was added to DNA reactant at an N/P ratio (amine group (N): phosphate group (P) = 4:1) in 0.3 mL DNase/RNase-free water for 30 min to form a stable complex. Then, the PLL/DNA reactant complex was mixed with 60 mg of PLGA-PEG-FA dissolved in 2 mL chloroform (organic phase) using a microtip probe sonicator at 4 °C for 1 min to formation of a primary (w/v) emulsion. The primary emulsion was further emulsified with a secondary aqueous phase (10 mL of 2.5% w/v PVA) at 4 °C for 2 min to form a secondary (W1/O/W2) emulsion. The resulting emulsion was immediately poured into the 40 mL of 2.5% (w/v) PVA and agitated using a magnetic stirrer overnight at room temperature until the

chloroform was completely evaporated. The synthesized nanovesicles were collected by centrifugation at 10,000g at 4 °C for 15 min, washed three times with deionized water and freeze-dried.

Characterization and morphology.

Hydrodynamic diameter, polydispersity, and zeta potential of the FA-nanovesicle was determined by DLS using a Zetasizer Nano ZS (Malvern, UK). Morphology of the FA-nanovesicle was investigated using scanning electron microscopy (Zeiss Merlin Compact, Germany) and transmission electron microscopy (JEM-2100, Japan).

Cell culture.

Human breast cancer cells (MCF-7) and cervical cancer cell (HeLa) were grown in Dulbecco's Modified Eagle's medium (DMEM, high glucose, Thermo Fisher, USA) containing 10% FBS and 1% penicillin/streptomycin at 37 °C in humidified 5% CO₂ atmosphere. Human normal lung fibroblast cells (MRC-5) were grown in MEM (Thermo Fisher, USA). Human breast normal cells (MCF-10A) were cultivated in complete growth medium (Procell Life Science & Technology Co., Ltd.). After reaching their 80-90% confluency, cells were treated with trypsin-EDTA (Thermo Fisher, USA) in order to subculturing. All cells were seeded into 12-well plates for flow cytometry analysis or 35 mm confocal dishes for confocal microscopy imaging.

Cell cytotoxicity evaluation.

MCF-7 and MCF-10A cells were seeded into 96-well plates at the density of 2×10^4 cells per well and incubated overnight until adherent, respectively. Then, the culture medium was discarded and incubated with fresh DMEM (200 μ L) containing different concentrations of the FA-modified nanovesicles. After incubation for 24 h, these cells were washed three times with PBS, followed by incubation with 100 μ L of MTT solution (1 mg mL⁻¹ in PBS) for 4 h in a culture incubator. After that, the supernatant medium was carefully removed and the formazan crystals were dissolved in 150 μ L

DMSO with gently shaking for 15 min. The absorbance at the wavelength of 490 nm was measured with a microplate reader (Thermo Scientific). The cell viability was calculated using the following equation:

$$\text{Cell Viability} = (\text{OD}_{\text{Treated}} - \text{OD}_{\text{Blank}}) / (\text{OD}_{\text{Control}} - \text{OD}_{\text{Blank}})$$

Cellular uptake assays.

Confocal laser scanning microscopy (CLSM) and flow cytometric assay were employed to investigate the cellular uptake. To investigate the receptor-mediated endocytosis, MCF-7, MCF-10A, and HeLa cells were pretreated either with or without excess free FA (1 mM) for 30 min, then washed three times with cold PBS. These cells were further incubated with FA-nanovesicle for 3 h. To evaluate the uptake mechanism of the FA-nanovesicle, MCF-7 cells were pretreated with NaN₃ (ATP inhibitor, 10 mM), chlorpromazine (inhibitor of clathrin-mediated endocytosis, 10 μg mL⁻¹), wortmannin (inhibitor of micropinocytosis, 5 μg mL⁻¹), nystatin (inhibitor of lipid raft-caveolae endocytosis, 2.5 μg mL⁻¹) for 30 min in a cell culture incubator, respectively. Then, these cells were washed three times with PBS, followed by incubation with the FA-nanovesicles for 3 h. For the CLSM assay, cells were stained with Hoechst 33342 for 15 min in a culture incubator. Cell imaging was carried out on the Leica TCS SP8 confocal laser scanning microscope (with the excitation wavelength of 488 nm for FAM and 405 nm for Hoechst 33342). For the anti-miRNA antisense inhibitor oligonucleotide experiment, the anti-miR-21 inhibitor (0.1 nmol) was prepared in Opti-MEM (50 μL), and was then mixed with lipofectamine 3000 (3 μL) dispersed in Opti-MEM (50 μL) for 5 min. Subsequently, the prepared Opti-MEM transfection mixture was introduced into the plated MCF-7 cells for 2 h at 37°C, followed by transfection and incubation with the nanovesicle system for 4 h. For quantitative analysis of the uptake of the FA-nanovesicles, cells were trypsinized and suspended in 500 μL cold PBS and analyzed by flow cytometry (BD FACSVerser, CA, USA).

Animal studies.

All animal experimental protocols were approved by the Institutional Animal Care and Use Committee of the Animal Experiment Center of Wuhan University (Wuhan, China). Four- to six-week-old female BALB/c nude mice were purchased from Charles River Company and raised in a specific pathogen-free grade laboratory according to guidelines for laboratory animals established by the Wuhan University Center for Animal Experiment/A3-Lab. All animals were housed with a 12 h light/dark cycle at 22 °C, 40% relative humidity, and food and water *ad libitum*.

Hemocompatibility Assay.

Fresh blood was obtained from BALB/c mouse, followed by centrifugation at 1000 g for 5 min at 4 °C. The RBCs were then washed several times with cold PBS until the supernatant was colorless. After that, 3% RBCs were mixed with the FA-nanovesicle with different concentrations with a total volume of 500 μ L. RBCs incubated with PBS and deionized water (DI) were used as negative and positive control, respectively. After incubation for 4 h at 37 °C, the solution was centrifuged at 1000g for 5 min and the absorbance spectra of the supernatant were measured at 570 nm. Hemolysis percentage was calculated according to the following formula:

$$\text{Hemolysis (\%)} = (A_{\text{sample}} - A_{\text{negative}}) / (A_{\text{positive}} - A_{\text{negative}}) \times 100\%$$

For SEM analysis of the RBCs, the RBCs were fixed by 2.5% glutaraldehyde for 30 min at 4 °C. Then, the RBCs were dehydrated with ethanol (15%, 30%, 40%, 50%, 70%, 80%, 90%, 100%) for 5 min orderly. Finally, the RBCs suspensions were dropped onto silicon slice and coated with Pt before viewing under a scanning electromicroscope (SEM, Hitachi, Japan).

***In vivo* imaging.**

MCF-7 cells (2.0×10^6) mixed with an equal volume of Matrigel (Corning), were orthotopically injected into the third mammary fat pad of female nude mice. When the tumour size reached $\sim 100 \text{ mm}^3$, as determined using digital calipers, the mice received intravenously injections of LCC-packaged FA-nanovesicle, H₁-mutant LCC-packaged

FA-nanovesicle, H₁-expelled LCC-packaged FA-nanovesicle or anti-miR-21 pretreated LCC-packaged FA-nanovesicle. At a given time point, whole-body imaging was investigated *via* an IVIS imaging system. Meanwhile, mice were injected with free DNA reactants, LCC-package nanovesicle, or LCC-packaged FA-nanovesicle through a tail vein. For biodistribution analysis, the mice were euthanized at the indicated time points post-injection and the tumours and major organs were harvested.

Detection of PDCD4 and PTEN protein levels in tumours:

For western blot analysis, the tumour tissues were lysed using RIPA lysis buffer (Beyotime, China) and centrifuged at 12, 000 g for 15 min at 4 °C. The supernatants were carefully collected and quantified *via* a BCA protein assay kit (Beyotime, China), separated by SDS-PAGE, and then transferred into the PVDF membrane. After blocking with QuickBlock™ (Beyotime, China) for 30 min, the blots were incubated with the primary antibodies (rabbit-PTEN: 1:1000; rabbit-PDCD4: 1:1000) in a blocking buffer at 4 °C overnight. Then, the PVDF membrane was washed three times with TBST for 5 min each time, followed by incubation at room temperature for 1 h with diluted secondary antibody (HRP-goat anti-rabbit: 1:2000) in TBST. Following additional washed three times with TBST, these membranes were then incubated with ECL substrate (Bio-Rad) and immediately detected using a ChemiDoc with Image Lab software (Bio-Rad).

Table S1. Sequences of the oligonucleotides for miRNA-responsive LCC amplifier

Name	Sequence (5'-3')
H ₁	TCA ACA TCA GTC TGA TAA GCT AAG TGT TCC TAA TAG CTT ATC AGA CTG AAA AAA CAA TGA CCG GTC ATT G
H _{1c}	TCA ACA TCA GTC TGA TAA GCT AAG TGT TCC TAA TAG CTT ATC AGA CTG AGA TCG CAG ACT CGA TC
H ₂	FAM -CTG ATA AGC TAT TAG GAA CAC TAC TGA TGT TGA AGT GTT CCT AAT AGC TGT AAC TCC GGA GTT AC-TAMRA
H ₃	TTA GGA ACA CTT CAA CAT CAG TTA GCT TAT CAG ACT GAT GTT GAA GTG TAA AAA GAT ACG CAT GCG TAT C
H _{3c}	TTA GGA ACA CTT CAA CAT CAG TTA GCT TAT CAG ACT GAT GTT GAA GTG TGA TAC GCA ACA GTA TC
miR-21	UAG CUU AUC AGA CUG AUG UUG A
miR-144	UAC AGU AUA GAU GAU GUA CU
Let-7a	UGA GGU AGU AGG UUG UAU AGU U
miR-429	UAA UAC UGU CUG GUA AAA CCG U
miR-155	UUA AUG CUA AUC GUG AUA GGG GU
1-Mut	UUA AUG CGA AUC GUG AUA GGG GU
2-Mut	UUA AUG CGA AUC GCG AUA GGG GU
3-Mut	UUA AUG CGA AUC GCG AUA GAG GU
anti-miR-21	mUmCmA mAmCmA mUmCmA mGmUmC mUmGmA mUmAmA mGmCmU mA

mN = 2'-O-Me RNA base

The nucleic acid bases marked in blue represent the symmetrical sequence

The bold italic nucleotides of mutant (mut) indicates the mismatched sequence

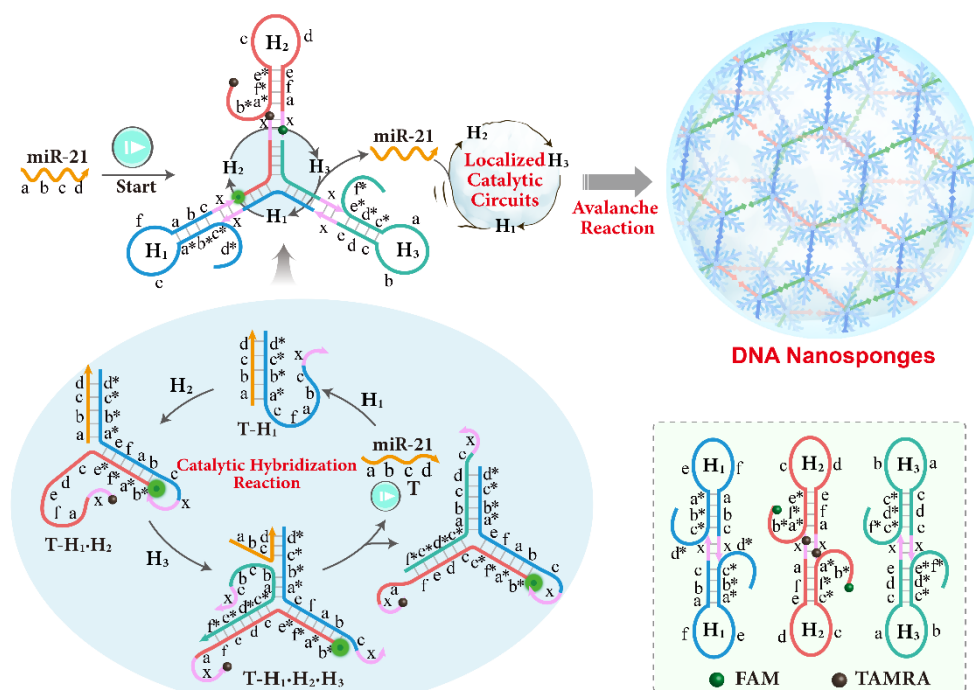


Figure S1. Stimulus-responsive assembly of DNA nanostructures by catenated DNA reactants. MiR-21 catalyzed the formation of the Y-shaped $H_1 \cdot H_2 \cdot H_3$ triplex that grafted with the self-supplemented scaffold-to-template, which leads to forming the advanced DNA architectures by the localized catalytic hybridization reaction for amplified fluorescence detection of the analyte.

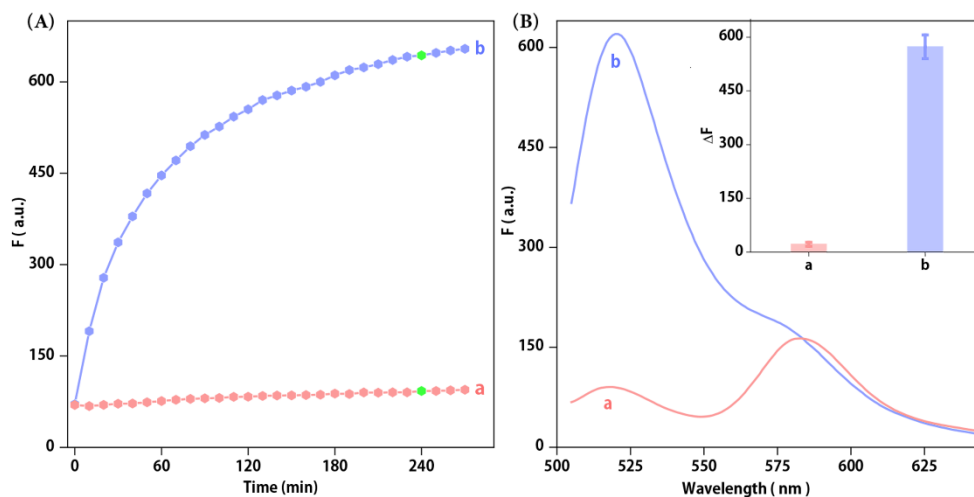


Figure S2. The feasibility of the miR-21-powered localized catalytic hybridization reaction. (A) Time-dependent fluorescence changes (at $\lambda=520$ nm) generated by the LCC system in the absence of miR-21 (a) and upon analysis of 100 nM miR-21 (b). (B) Fluorescence spectra generated by the LCC system are shown in Figure S2A for a fixed time interval of 240 min. Inset: summary of the results of fluorescence spectra at $\lambda=520$ nm. Data represent the mean \pm s.d. from three independent experiments.

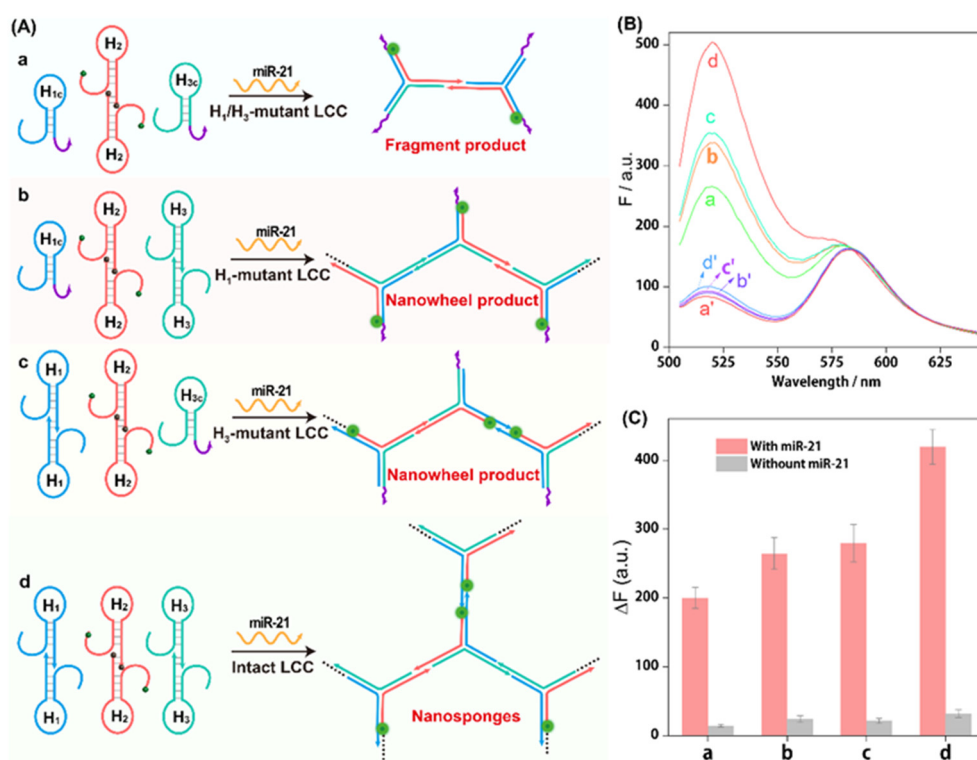


Figure S3. Comparison of the self-assembly efficiency for conventional DNA reactants and interconnecting catenated DNA reactants. (A) The scheme for miR-21-responsive hybridization behaviors at different conditions. Herein, the original symmetrical sequence of H₁ and H₃, a key transducing fragment of the LCC system, was replaced with a random sequence to generate H_{1c} and H_{3c}. (B) Fluorescence spectra generated by the LCC system outlined in Figure S3A: (a) miR-21+H₁/H₃-mutant LCC; (a') H₁/H₃-mutant LCC; (b) miR-21+H₁-mutant LCC; (b') H₁-mutant LCC; (c) miR-21+H₃-mutant LCC; (c') H₃-mutant LCC; (d) miR-21+intact LCC; (d') intact LCC. (C) Summary of the results of fluorescence spectra at $\lambda=520$ nm. The system consisting of 200 nM hairpins was reacted at room temperature in HEPES buffer (10 mM HEPES, 1 M NaCl, 50 mM MgCl₂, pH 7.2) for a fixed time interval of 240 min. Data represent the mean \pm s.d. from three independent experiments.

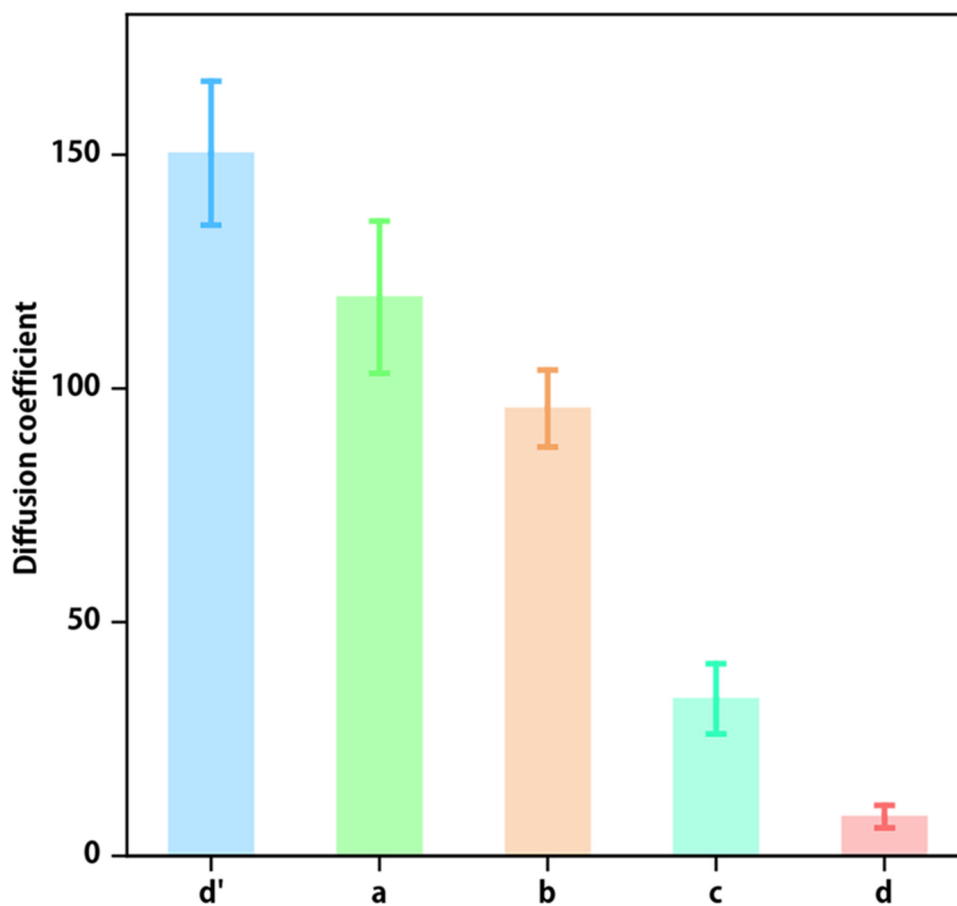


Figure S4. Characteristic diffusion coefficient (D) of the LCC system as shown in Figure 2C: (a) miR-21+H₁/H₃-mutant LCC; (b) miR-21+H₁-mutant LCC; (c) miR-21+H₃-mutant LCC; (d) miR-21+intact LCC; (d') intact LCC. Data represent the mean \pm s.d. from five independent experiments.

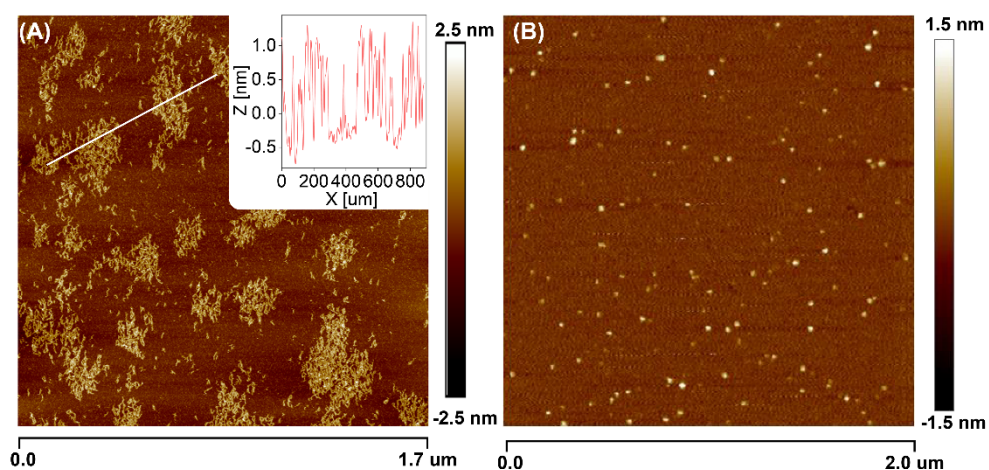


Figure S5. AFM characterization of the LCC system. (A) The H₁-mutant LCC system-driven supramolecular dsDNA nanowires and corresponding cross-section analysis. (B) The intact LCC system without the presence of the promoter.

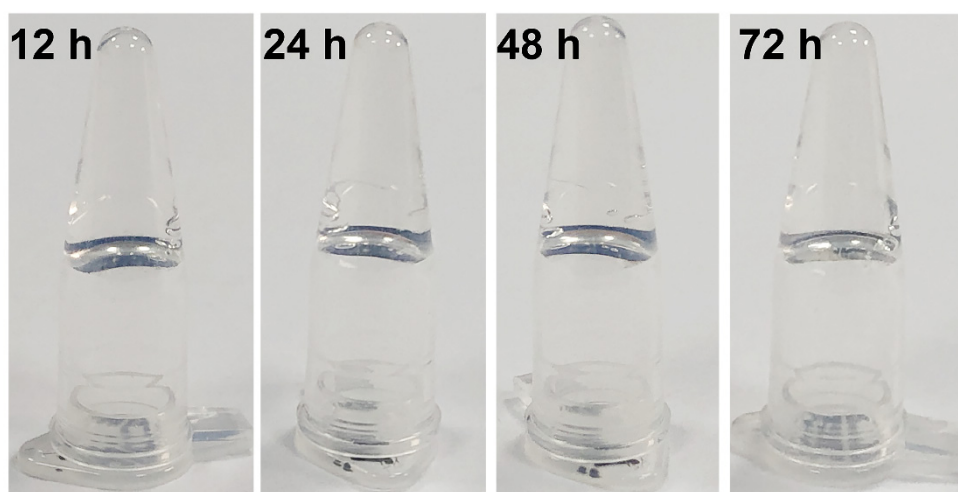


Figure S6. The stability of the DNA hydrogels.

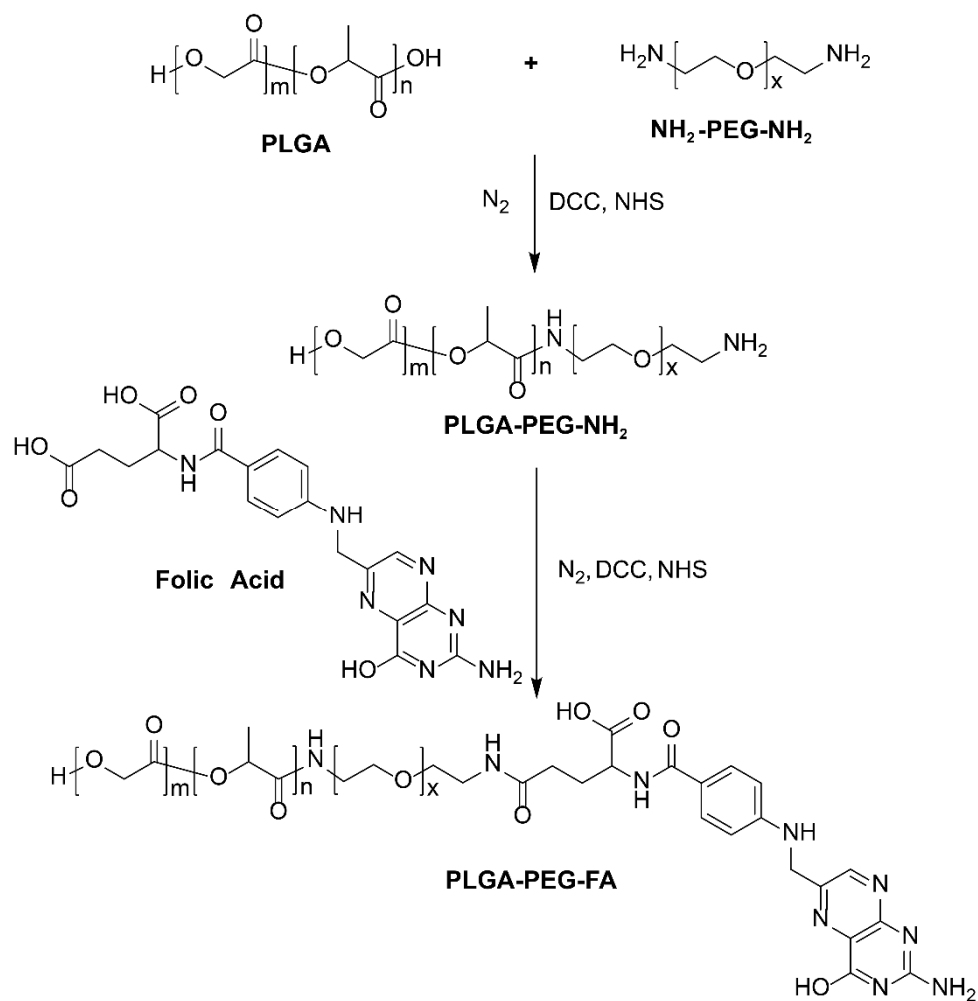


Figure S7. Schematic illustration the synthesized PLGA-PEG-FA.

Supporting Information

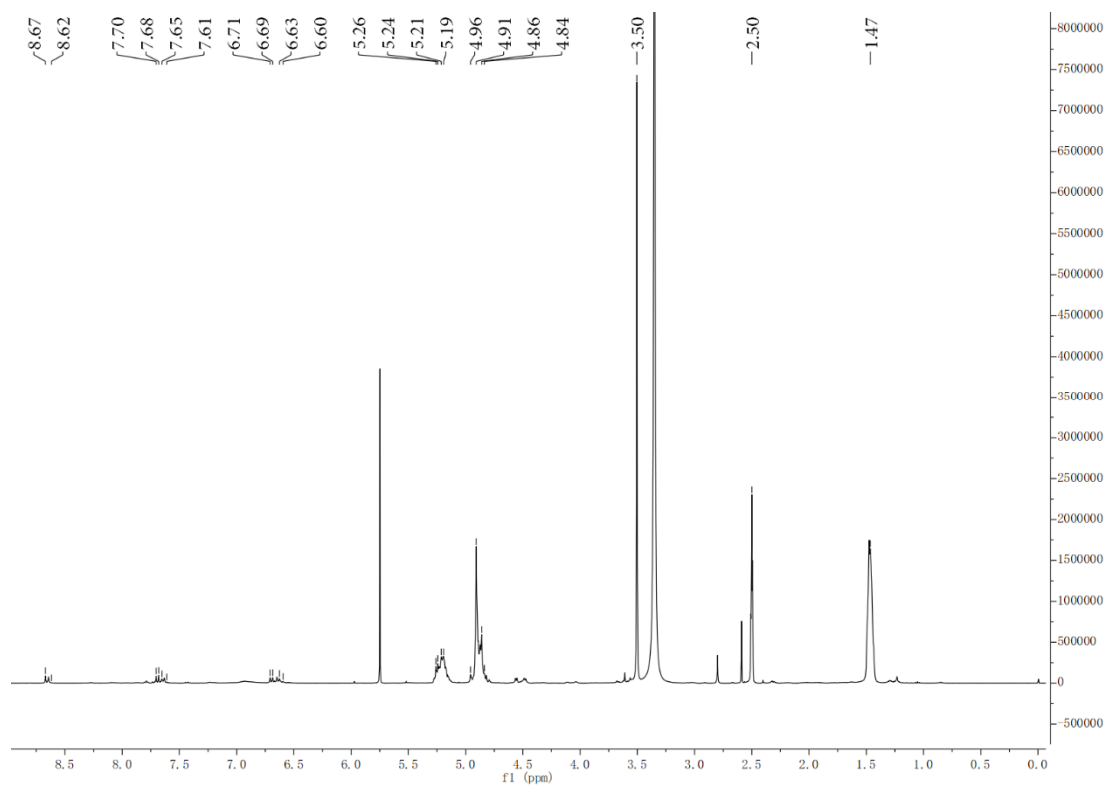


Figure S8. ¹H NMR spectra of synthesized FA-PLGA polymer.

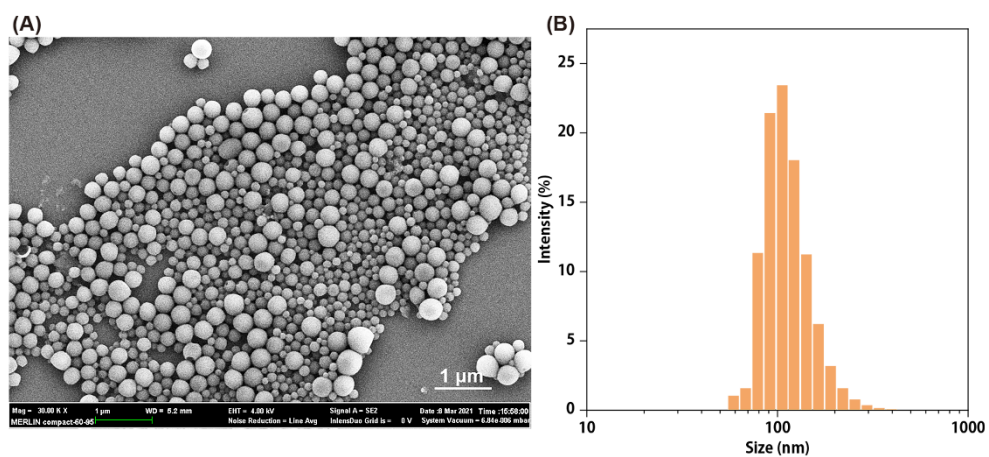


Figure S9. Stability evaluation. (A) SEM image and (B) Hydrodynamic diameter measurement of the FA-nanovesicles in DMEM with 10% serum for 24 h.

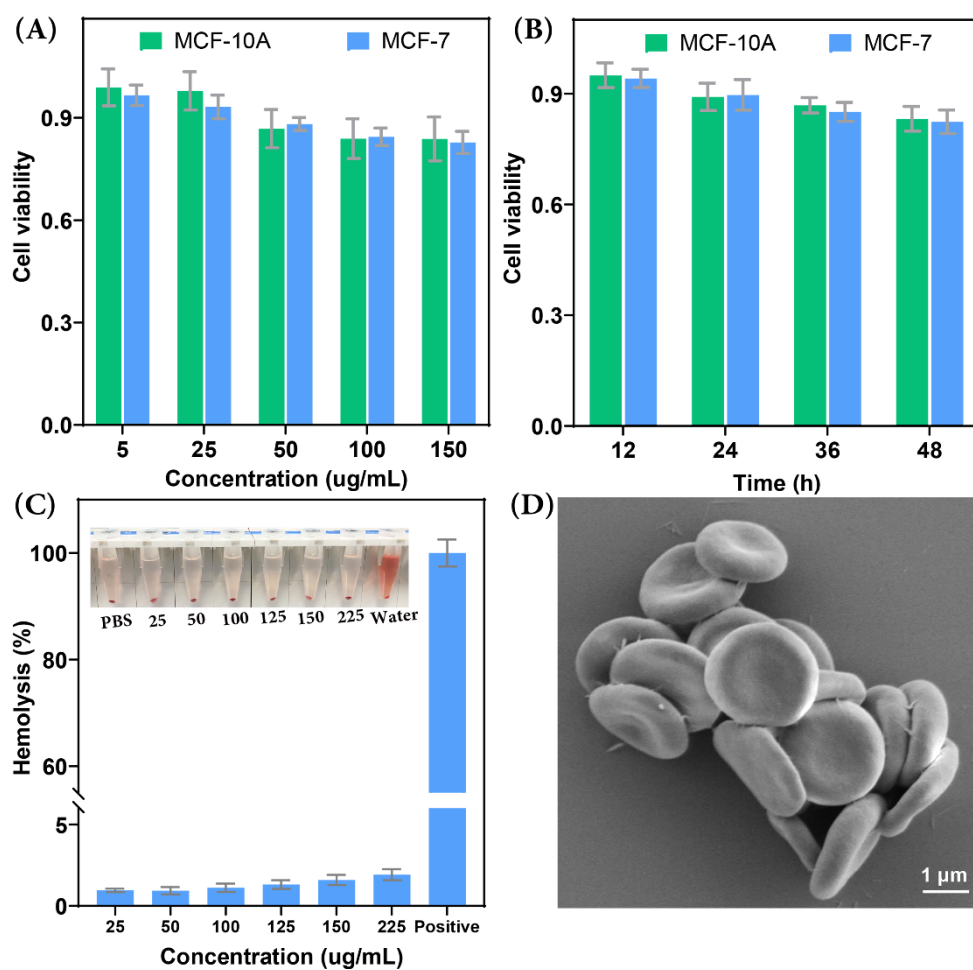


Figure S10. The biocompatibility evaluation of the FA-nanovesicles. (A) Cell viability of MCF-10A and MCF-7 cells incubated with various concentrations of the FA-nanovesicles for 24 h, respectively. (B) Cell viability of MCF-10A and MCF-7 cells after various incubation times with 125 $\mu\text{g}/\text{mL}$ FA-nanovesicles. (C) Hemolytic analysis of mouse red blood cells after treatment with the FA-nanovesicles. Water and PBS were used as positive control and negative control, respectively. (D) SEM images for RBC morphology after treatment with 300 $\mu\text{g}/\text{mL}$ FA-nanovesicles for 4 h. Data represent the mean \pm s.d. of five independent replicates.

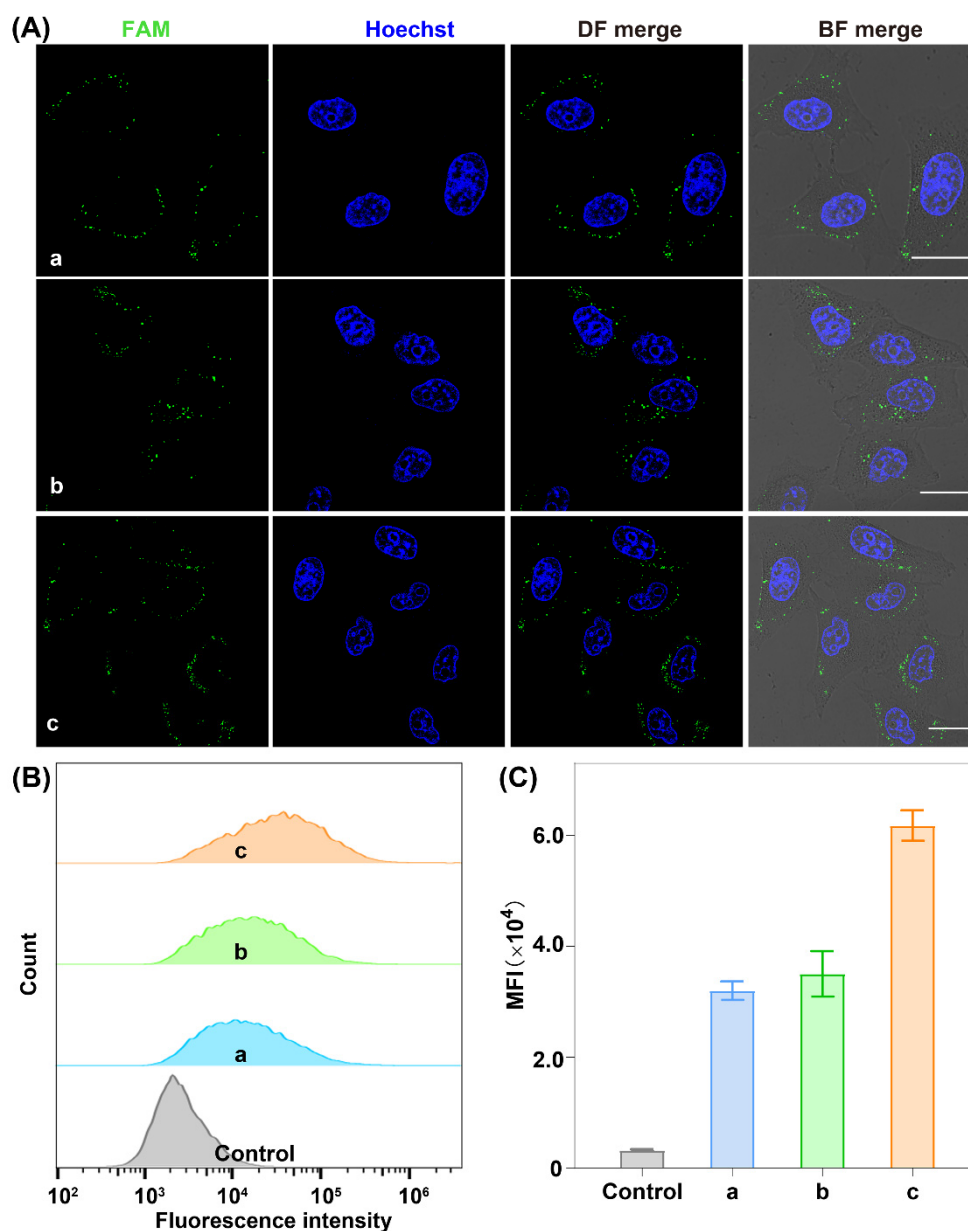


Figure S11. Inhibition analysis of FA-receptor mediated endocytosis in FR-positive MCF-7 cells. (A) Confocal microscopy characterization and (B, C) the corresponding flow cytometry quantification of the internalized nanovesicles (a), free FA pre-treated FA-nanovesicles (b), and FA-nanovesicles (c). The cell nuclei were stained with Hoechst 33342 (blue). Scale bar: 20 μ m. Data represent the mean \pm s.d. of three independent replicates.

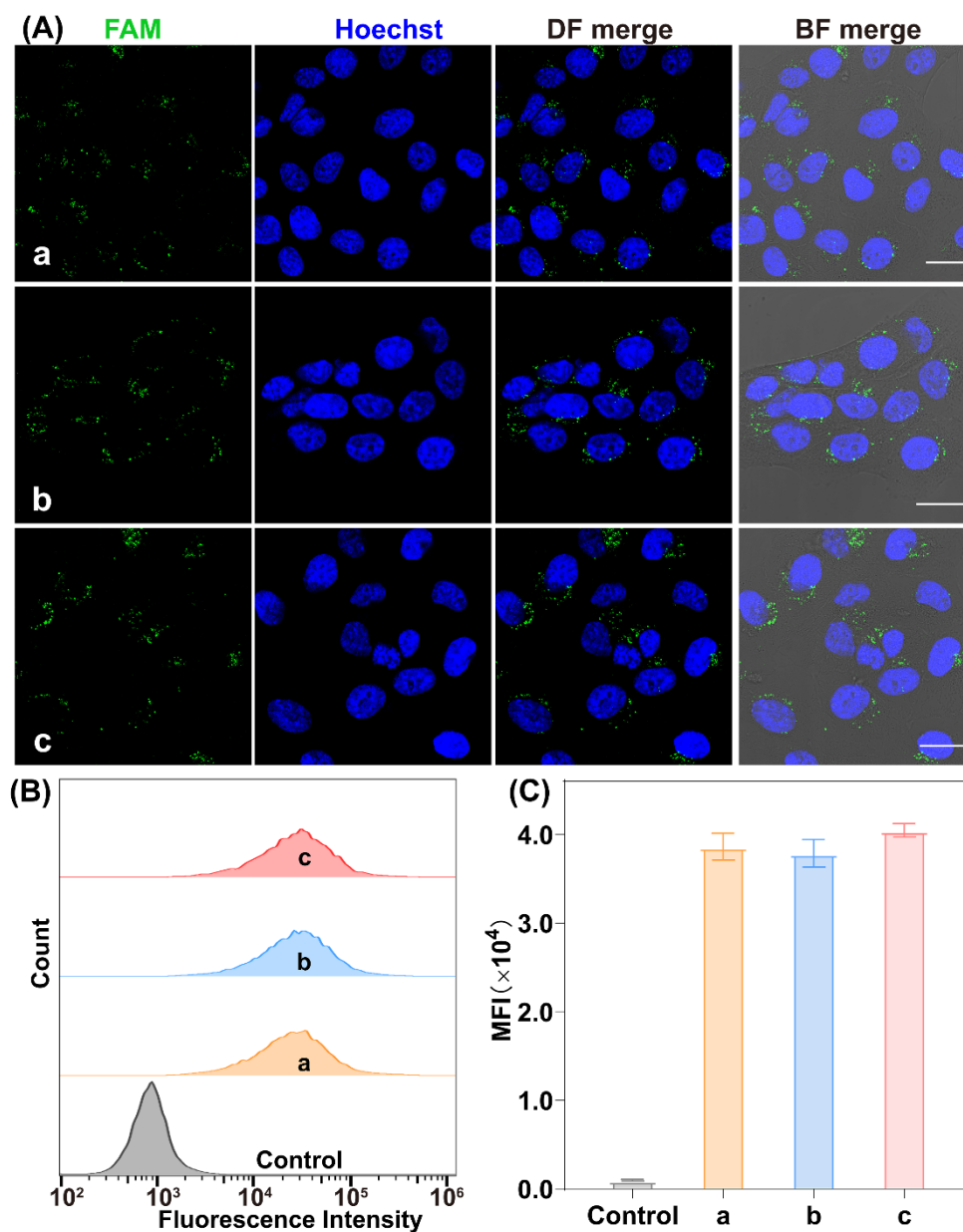


Figure S12. Inhibition analysis of FA-receptor mediated endocytosis in FR-negative MCF-10A cells. (A) Confocal microscopy characterization and (B, C) the corresponding flow cytometry quantification of the internalized nanovesicles (a), free FA pre-treated FA-nanovesicle system (b), and FA-nanovesicle system (c). The cell nuclei were stained with Hoechst 33342 (blue). Scale bar: 20 μ m. Data represent the mean \pm s.d. of three independent replicates.

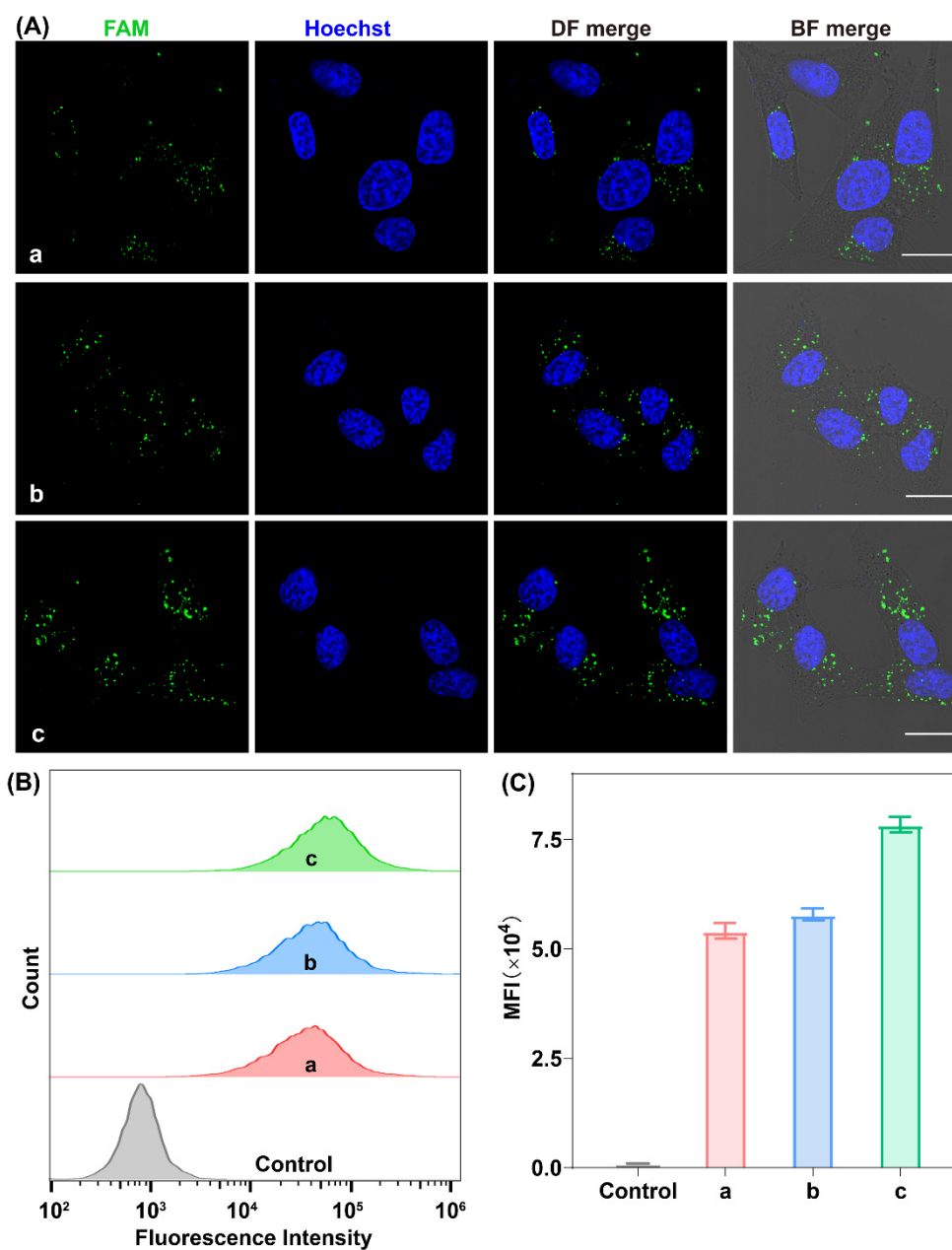


Figure S13. Cellular uptake of the nanovesicles in FR-positive HeLa cells after 3 h incubation. (A) Confocal microscopy characterization and (B, C) the corresponding flow cytometry quantification of the internalized nanovesicles (a), free FA pre-treated nanovesicles (b), and FA-nanovesicles system (c). The cell nuclei were stained with Hoechst 33342 (blue). Scale bar: 20 μm . Data represent the mean \pm s.d. of three independent replicates.

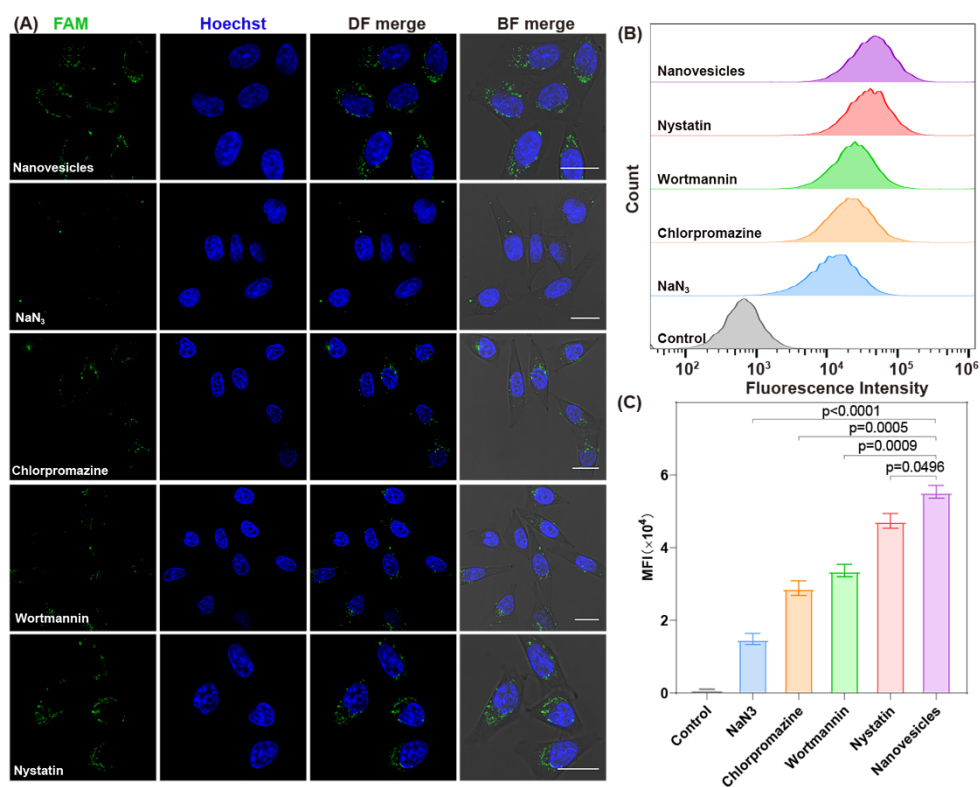


Figure S14. Cellular uptake mechanism of the FA-nanovesicles. (A) CLSM analysis of the internalized FA-nanovesicles in MCF-7 cells that were pre-treated with different endocytosis inhibitors. The cell nuclei were stained with Hoechst 33342 (blue). Scale bar: 20 μ m. (B, C) Quantification by analytical flow cytometry of the internalization of FA-nanovesicles in the presence of several small-molecule inhibitors. Data represent the mean \pm s.d. of three independent replicates. Statistical significance is calculated by one-way ANOVA followed by Tukey's post hoc test.

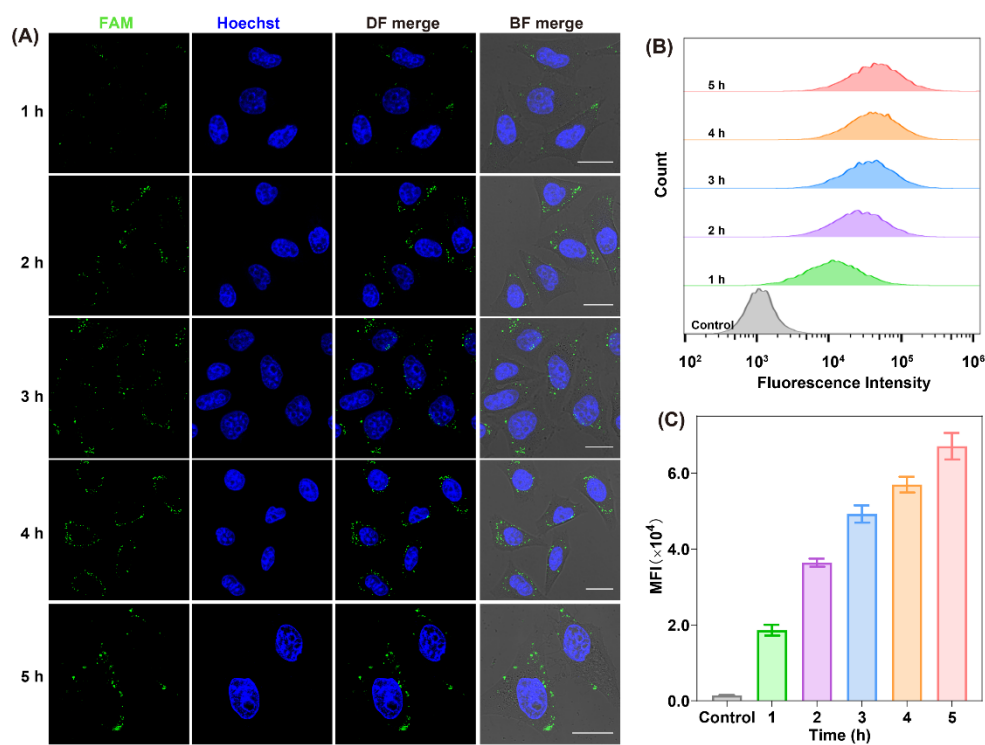


Figure S15. Optimization of incubation time of the FA-nanovesicles in living MCF-7 cells. (A) CLSM analysis of the FA-nanovesicles that were incubated with MCF-7 cells for different time intervals. The cell nuclei were stained with Hoechst 33342 (blue). Scale bar: 20 μm . (B) Flow cytometric analysis and (C) the corresponding mean fluorescence intensity (MFI) in cells incubated with the FA-nanovesicles for varied durations. Data represent the mean \pm s.d. of three independent replicates.

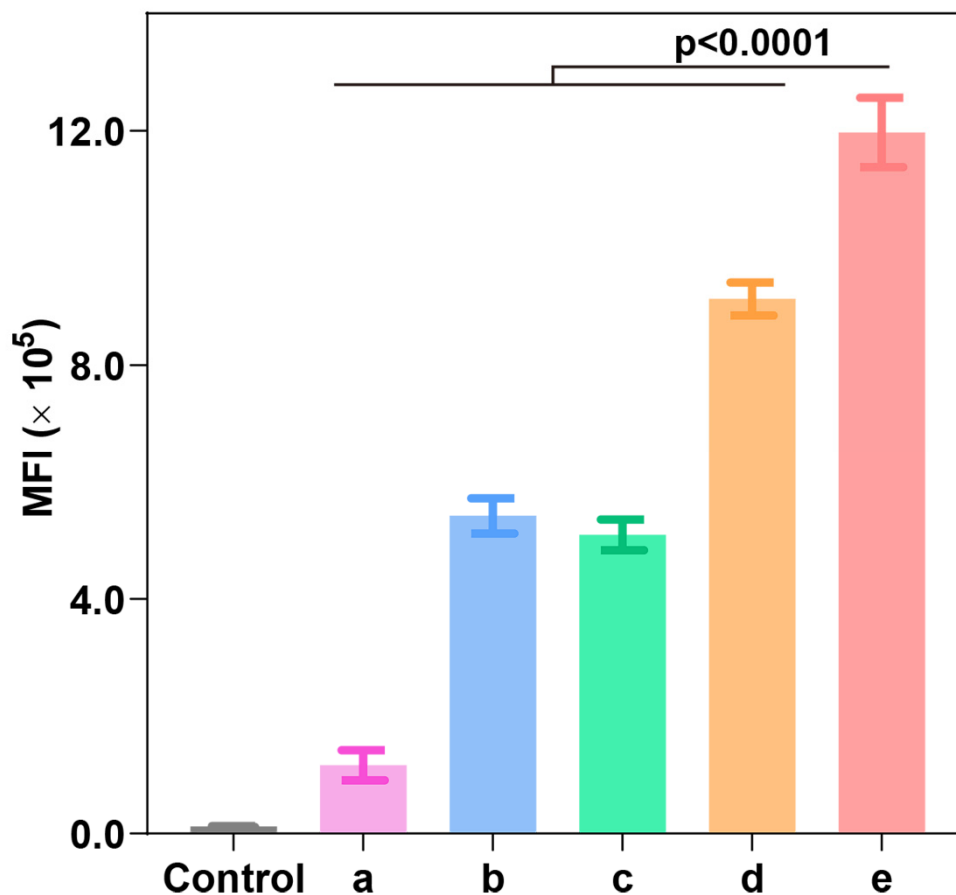


Figure S16. Quantitative analysis of the intracellular mean fluorescence intensity (MFI) that were respectively incubated with anti-miR-21-pretreated LCC system (a), H₁/H₃-mutant LCC system (b), H₁-mutant LCC system (c), H₃-mutant LCC system (d), and intact LCC system (e). Data represent the mean \pm s.d. of three independent replicates. Statistical significance is calculated by one-way ANOVA followed by Tukey's post hoc test.

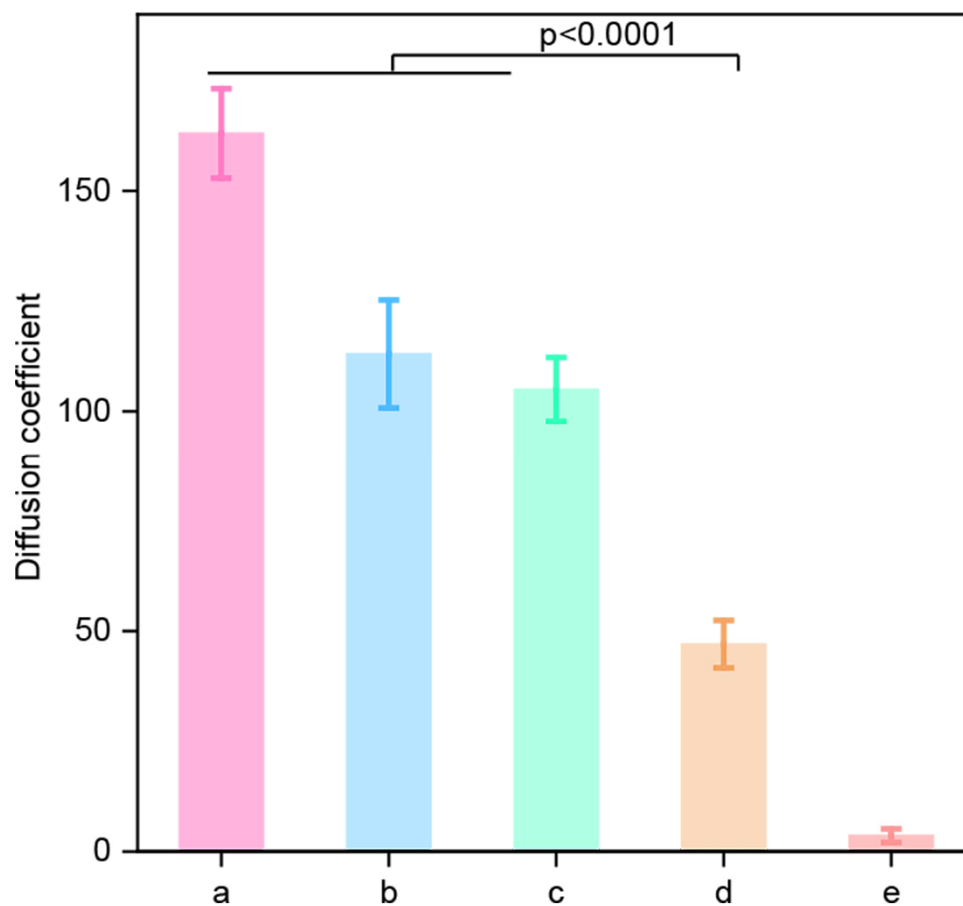


Figure S17. Characteristic diffusion coefficient (D) assay in MCF-7 cells that were respectively incubated with anti-miR-21-pretreated LCC system (a), H₁/H₃-mutant LCC system (b), H₁-mutant LCC system (c), H₃-mutant LCC system (d) and intact LCC system (e). Data represent the mean \pm s.d. of five independent experiments. Statistical significance is calculated by one-way ANOVA followed by Tukey's post hoc test.

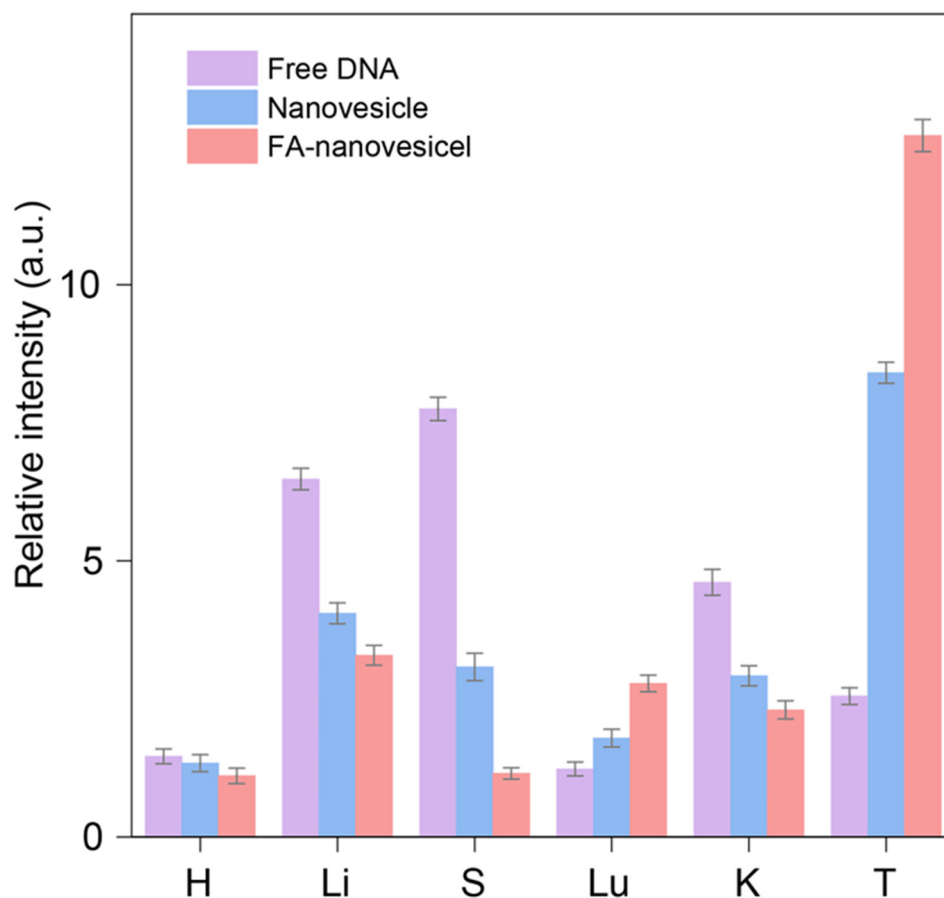


Figure S18. The signal intensities of the major organs and tumours after free DNA, LCC-packaged nanovesicle, or LCC-packaged FA-nanovesicle for 16 h. H, heart; Li, Liver; S, spleen; Lu, lung; K, kidney; T, tumour. Data represent the mean \pm s.d. of three independent replicates.

Supporting Information

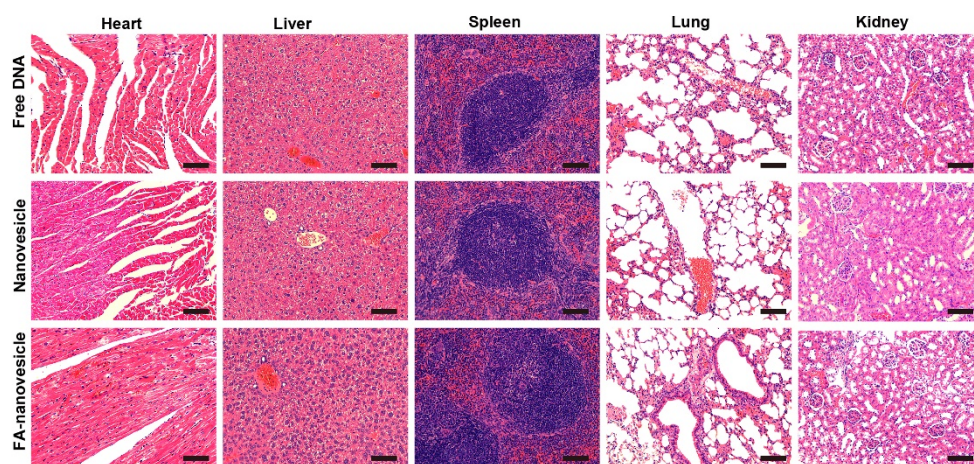


Figure S19. H&E-stained tissue sections of heart, liver, spleen, lung, and kidney, acquired at 24 h after various treatments. All scale bars are 200 μm .

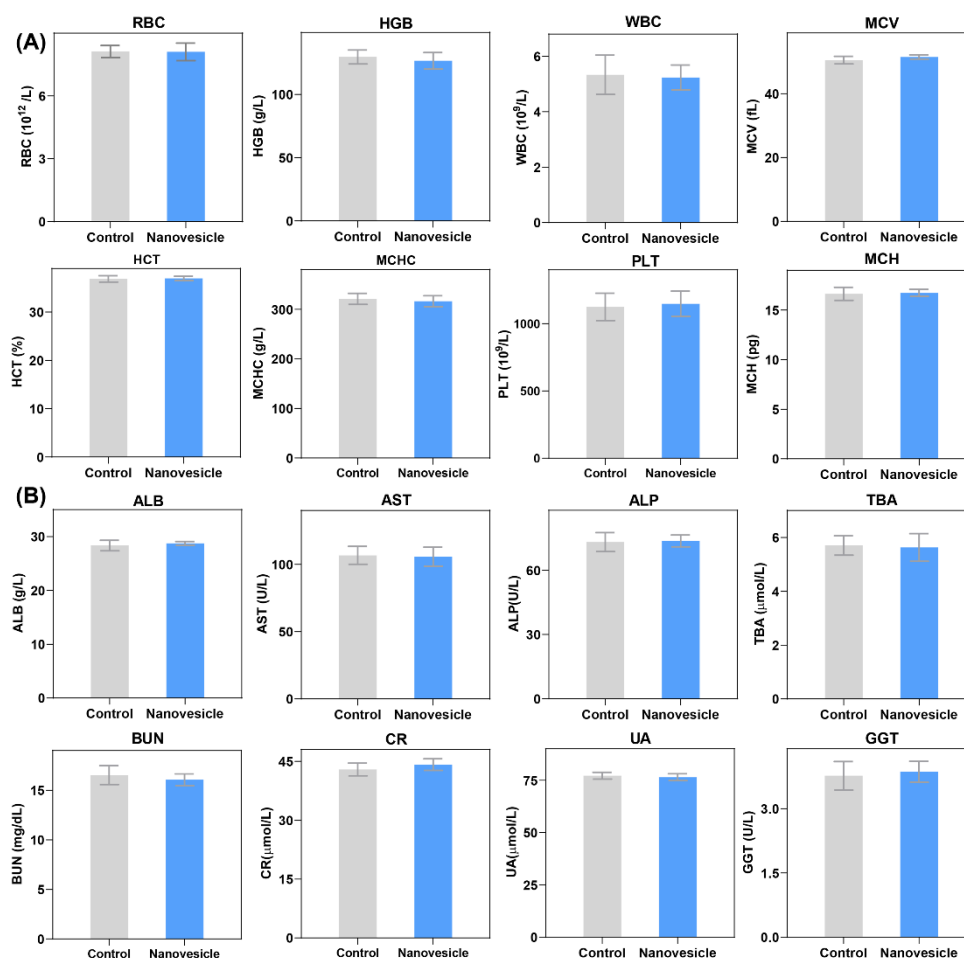


Figure S20. Biosafety evaluation of the FA-nanovesicles in vivo. (A) Whole blood cell analysis of the mice after 24 h post intravenous injection FA-nanovesicles. The tested indexes include blood cells (RBC), hemoglobin (HGB), white blood cells (WBC), mean corpuscular volume (MCV), hematocrit (HCT), mean corpuscular hemoglobin concentration (MCHC), platelets (PLT), mean corpuscular hemoglobin (MCH). (B) Hepatic and renal functions analysis of the intravenously injected mice with FA-nanovesicles after 24 h. The tested indexes include albumin (ALB), aspartate aminotransferase (AST), alkaline phosphatase (ALP), total bile acid (TBA), aspartate aminotransferase (BUN), serum creatinine (CR), uric acid (UA), gamma-glutamyltransferase (GGT). Data represent the mean \pm s.d. of three independent replicates.

References

- [1] El-Gogary, R. I., Rubio, N., Wang, J. T., Al-Jamal, W. T., Bourgognon, M., et al. *ACS nano*, **2014**, 8, 1384-1401.
- [2] S. Jain, V. V. Rathi, A. K. Jain, M. Das, C. Godugu, *Nanomedicine* **2012**, 7, 1311-1337.
- [3] J. H. Kim, Y. W. Noh, M. B. Heo, M. Y. Cho, Y. T. Lim, *Angew. Chem., Int. Ed.* **2012**, 51, 9670-9673.